Heliyon 10 (2024) e25267

Contents lists available at ScienceDirect

Heliyon

journal homepage: www.cell.com/heliyon

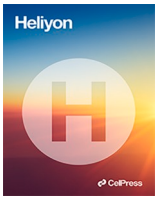

Research article

# Xingnaojing injection alleviates cerebral ischemia/reperfusion injury through regulating endoplasmic reticulum stress in Vivo and in Vitro

Xinglu Dong [a,b,d,1], Chuanpeng Li [a,b,c,1], Yaoyao Yao [a,b,c], Fengzhi Liu [a,b,c], Ping Jiang [a,b,d], Ying Gao [a,b,c,d,*]

[a] *Department of Neurology, Dongzhimen Hospital, Beijing University of Chinese Medicine, Beijing, China*
[b] *Institute for Brain Disorders, Beijing University of Chinese Medicine, Beijing, China*
[c] *Chinese Medicine Key Research Room of Brain Disorders Syndrome and Treatment of the National Administration of Traditional Chinese Medicine, Beijing, China*
[d] *Key Laboratory of Chinese Internal Medicine of Ministry of Education and Beijing, Dongzhimen Hospital Affiliated to Beijing University of Chinese Medicine, Beijing, China*

ARTICLE INFO

*Keywords:*
Xingnaojing injection
Traditional Chinese medicine
Endoplasmic reticulum stress
Apoptosis
Ischemic stroke
Cerebral ischemia-reperfusion injury

ABSTRACT

*Background:* Xingnaojing (XNJ) injection, an extract derived from traditional Chinese medicine, is commonly used to treat ischemic stroke (IS). Previous studies have shown that XNJ has the ability to alleviate apoptosis in cerebral ischemia-reperfusion injury. However, the potential mechanisms have not been clarified.

*Objective:* To identify the neuroprotective effect of XNJ and explore whether XNJ inhibits cell apoptosis associated with endoplasmic reticulum stress (ERS) after IS.

*Methods:* In this study, cultured hippocampal neurons from mouse embryos and Sprague-Dawley rats were assigned randomly to four groups: sham, model, XNJ, and edaravone. The treatment groups were administered 2 h after modelling. Neurological deficit scores and motor performance tests were performed after 24 h of modelling. Additionally, pathomorphology, cell apoptosis and calcium content were evaluated. To ascertain the expression of ERS proteins, western blotting and polymerase chain reaction were employed.

*Results:* The results indicated that XNJ treatment resulted in a notable decrease in infarct volume, apoptosis and missteps compared with the model group. XNJ also exhibited improvements in neurological function, grip strength and motor time. The calcium content significantly reduced in XNJ group. The XNJ administration resulted in a reduction in the levels of proteins associated with ERS including CHOP, GRP78, Bax, caspase-12, caspase-9, and cleaved-caspase-3, but an increase of the Bcl-2/Bax ratio. Furthermore, the downregulation of mRNA expression of CHOP, GRP78, caspase-12, caspase-9, and caspase-3 was confirmed in both cultured neurons and rat model.

*Conclusion:* These findings suggest that XNJ may alleviate apoptosis by modulating the ERS-induced apoptosis pathway, making it a potential novel therapeutic approach for ischemic stroke.

* Corresponding authorNo. 5, Haiyuncang Lane, Dongcheng District, Beijing, 100700, China.
*E-mail address:* gaoying973@163.com (Y. Gao).

[1] These authors have made equal contributions to this project and share the position of first author.

https://doi.org/10.1016/j.heliyon.2024.e25267
Received 19 September 2023; Received in revised form 23 January 2024; Accepted 23 January 2024
Available online 24 January 2024

## 1. Introduction

Stroke has been the primary contributor to disability and the second most common reason for death around the world, with approximately five million cases occurring annually in China alone, thereby posing a significant threat to human well-being and imposing substantial economic and medical burdens [1,2]. Ischemic stroke accounts for about 70 % of all stroke cases [3]. Reestablishing blood flow through reperfusion is a crucial therapeutic approach for managing ischemic stroke [4]. Nonetheless, in certain instances, reperfusion of cerebral blood flow not only fails to alleviate disease progression but also exacerbates damage to ischemic brain tissues, recognised as cerebral ischemia-reperfusion injury (CIRI) [5–7]. Neurological deficits in ischemic stroke are due to a series of complex pathological processes, of which CIRI is the core pathological link [8]. Thus, attenuating CIRI is essential for the management of acute IS.

The documentation of the mechanism of CIRI remains insufficient in academic literature. Several studies suggest that CIRI is implicated in various detrimental processes such as oxidative stress, cell apoptosis, calcium overload, excitatory amino acid toxicity, disruption of the blood brain barrier and inflammatory response [9]. Among these pathological processes, cell apoptosis is a significant consequence of oxidative stress, calcium overload, and inflammatory response [10]. Additionally, cell apoptosis plays a crucial function in the formation of the ischemic penumbra surrounding the central necrotic core, serving as a pivotal process that can be mitigated to limit the expansion of the infarct area [11,12]. Consequently, it is vital to ameliorate CIRI through regulating cell apoptosis.

The signal transduction pathways involved in cell apoptosis encompass both mitochondrial-mediated pathways and pathways mediated by endoplasmic reticulum stress (ERS) and death receptors [13,14]. ERS, a mechanism of apoptosis that has been recently discovered, is essential for the proper folding and functioning of numerous secretory and membrane proteins within the endoplasmic reticulum [15]. Following hypoxic-ischemic injury and calcium overload, disruptions in endoplasmic reticulum homeostasis and an accumulation of unfolded proteins within the organelle are observed in neurons [16–18]. When the quantity of unfolded proteins surpasses the capacity of the endoplasmic reticulum to manage the load, cells have the ability to initiate an unfolded protein response in order to cope with the consequences of stressful conditions and restore the cellular environment from protein folding, called ERS [19]. During ERS, the interaction between GRP78 and PKR-like endoplasmic reticulum kinase (PERK), activated transcription factor 6 (ATF6), and Inositol-requiring protein 1 (IRE1) is disrupted, and the stress-sensing domains of each transmembrane protein activate stress signal. Consequently, the dissociation and up-regulation these proteins occur [20]. The induction of an intense or persistent ERS leads to the up-regulation of CHOP expression, which subsequently increases the expression of Bax/Bak and inhibits the expression of the anti-apoptotic protein Bcl-2. This results in a conformational change of Bax/Bak localized on the endoplasmic reticulum, ultimately causing damage to its integrity [21]. Caspase-12, primarily located in the endoplasmic reticulum and selectively activated by ERS, is considered a specific apoptotic mediator in the ERS apoptotic pathway. Caspase-12 initiates the classical apoptotic pathway of caspase family, and activates procaspase-9, which further activates procaspase-3, leading to apoptosis [15,22]. In addition, after acute ischemic stroke, the brain tissue in the lesion area is in a state of ischemia and hypoxia due to insufficient blood supply. The free radical content in the lesion tissue is significantly increased, affecting the calcium pump function on the endoplasmic reticulum membrane, thus gradually exhausting $Ca^{2+}$ in the endoplasmic reticulum and causing calcium overload in cytoplasm and mitochondria, which further induce ERS, causing cell apoptosis [23,24]. Thus, down-regulating apoptosis through suppressing ERS is a significant approach for alleviating cerebral ischemia/reperfusion injury.

Xingnaojing (XNJ) injection is composed of musk (Moschus), *Curcuma aromatica* Salisb [Zingiberaceae], *Gardenia jasminoides* J. Ellis [Rubiaceae] and Borneolum syntheticum [25]. Approved by the China Food and Drug Administration, it is extensively utilized during the acute stage of ischemic stroke [26]. Prior clinical studies have shown that XNJ improves neurological performance in brain injury and promotes rehabilitation of neurological function probably attributing to its anti-apoptotic function [27,28]. However, the anti-apoptotic mechanisms of XNJ in ischemic stroke have not been fully clarified. Hence, our present investigation aims to explore if ERS-triggered cell death plays a role in the neuroprotective properties of XNJ.

## 2. Materials and methods

### 2.1. Chemicals and reagents

Eadravone was provided by Nanjing Simcere Dongyuan Pharmaceutical Co., Ltd. (Nanjing, China). The XNJ injection was acquired from Wuxi Jiminkexin Shanhe Pharmaceutical Co., Ltd. (Wuxi, China). Antibodies to glyceraldehyde-3-phosphate dehydrogenase (GAPDH, 60004-1-Ig) and B-cell lymphoma-2 (Bcl2, 12789-1-AP) were purchased from Proteintech Group, Inc. (Rosemont, IL, USA). Antibodies to C/EBP homologous protein (CHOP, 2895) and cleaved-caspase-3 (9662S) were obtained from Cell Signaling Technology (Boston, MA, USA). Antibodies to Bcl2-associated X protein (Bax, ab32503), caspase-9 (ab184786), and caspase-12 (ab62484) were obtained from Abcam (Cambridge, UK). Secondary antibodies (HRP-conjugated Affinipure Goat Anti-Mouse IgG, SA00001-1; HRP-conjugated Affinipure Goat Anti-Rabbit IgG, SA00001-2) were purchased from Proteintech Group, Inc. (Rosemont, IL, USA).

### 2.2. Animals and ethics statement

Male Sprague-Dawley rats weighing between 250 and 300 g were obtained from Beijing Huafukang Biotechnology Co., Ltd, and all rats were housed in the Animal Barrier Laboratory of the Key Laboratory of Ministry of Education, Dongzhimen Hospital at a humidity

of 70 % at 23 ± 3 °C and on a 12 h light/dark cycle. All animals were offered with adequate water and food. All procedures for the care and experimentation of animals were carried out in compliance with the National Research Council's Guidelines for the Care and Use of Laboratory Animals. The Animal Ethics Committee of Dongzhimen Hospital affiliated with Beijing University of Chinese Medicine (registration and ethical approval number: 20–42 approved on November 20, 2020) granted approval for the experimentation protocols. Our efforts were focused on minimizing the quantity of animals utilized and guaranteeing their well-being throughout the experiments. Before operation, a 24-h fasting period was observed for all rats, during which they were permitted to consume water in their usual manner. Prior to commencing the modelling procedure, the rats were fully anesthetized. Lidocaine was applied at the site of the animal wounds during the surgical procedures. The modelling process was conducted in a serene and sterile environment. Once the modelling procedure was completed, the rats were positioned on temperature-controlled pad. Rats (n = 100) were randomly and equally assigned to four groups: sham, MCAO, XNJ, and edaravone, corresponding to the injection of physiological saline (2 mL/kg), physiological saline (2 mL/kg), XNJ injection (2 mL/kg), edaravone (2 mL/kg), respectively. XNJ injection and edaravone were separately intraperitoneal injected after 2 h of modelling.

### 2.3. Middle cerebral artery occlusion and reperfusion

Prior to the procedure, a 24-h fasting period was observed for all rats, during which they were permitted to consume water in their usual manner. The rats were anesthetized intraperitoneally with 1 % sodium phenobarbital. The temperature-controlled pad helped maintain a body temperature close to 37 °C. Then the midline of the neck was incised, and the carotid arteries, including the common, internal, and external ones, were carefully dissected. Through the external carotid artery stump, a nylon monofilament suture was inserted into the right internal carotid artery. After 90 min of obstruction, the monofilament nylon was dismantled to perform reperfusion [29]. The same method was used on the sham operation group except for insertion of the nylon thread. Once reviving, neurobehavioral score of each rat was assessed by the Longa standard neurological deficit score with the following score points: 0, no nerve injury symptoms; 1, failure to extend the left front claw; 2, levoversion; 3, left toppling; 4, failure to walk spontaneously or unconscious. Rat with the score of 2 or 3 was considered as a successful modelling.

### 2.4. Neurological deficiency score

Neurological functions were assessed using the modified neurological severity score (mNSS) following a 24-h period of brain ischemia-reperfusion injury. A researcher blind to grouping assessed mNSS from the four aspects of motion, feeling, balance and reflection: 0, no neurological deficiency; 1–6, mild neurological deficiency; 7–12, moderate neurological deficiency; 13–18, severe neurological deficiency.

### 2.5. Infarct volume assessment

Rats were anesthetized before euthanasia and brain extraction. These brains were dyed by 2,3,5-triphenyte-trazoliumchloride (TTC). Each brain was sliced into five coronal sections with a thickness of 2 mm, which were then incubated in a 2 % TTC at a temperature of 37 °C for a duration of 30 min. The normal tissue in the brain was stained red while infarction tissues displayed white. The infarction area was measured by image analysis system (image Pro Plus 6.0). To determine the size of the infarct, the sum of the ischemic areas of each slice was multiplied by their respective thickness. The formula used to normalize the infarct volume was (infarct volume/total volume) × 100 % [30].

### 2.6. Assessment of brain water content

Tissue sample of whole brain under wet weight was measured by analytical balance. Then, the tissue sample was dried by electric drying oven under 100 °C for 48 h, and its dry weight was immediately measured. The estimation of brain water content was calculated: (wet weight - dry weight)/wet weight × 100 % [31].

### 2.7. Motor performance tests

A grip strength test, a rotarod test, and a foot misplacement test were applied to determine motor activity and coordination after MCAO. The motor function was assessed in a blinding fashion.

#### 2.7.1. Grip strength test

A paw grip test apparatus (BIO-GS3; Panlab, Barcelona, Spain) was used to assess the grab force of anterior limbs. The procedure was as follows: the paw grip test apparatus was placed on a horizontal platform. The rat tails were lifted, and the forelimbs were placed on the grasping instrument sensing bar. After grasping the bar, their forelimbs were horizontally dragged backwards, until their forelimbs loosened. The paw grip test apparatus automatically recorded the maximum grip force during the grasping rod. The measurements were repeated on three occasions, and the maximum value was adopted and scored as the rat forelimb grip.

#### 2.7.2. Rotarod

Using the running wheels training method with a baseline acceleration mode on a rotarod apparatus (model LE8505; Panlab,

Barcelona, Spain), the rats were behaviorally trained for three days before modelling. Rats that did not fall off the running wheel for at least 60 s were eligible. Rats were scored by one independent experimenter who was unaware of the grouping. Behavioral tests were conducted on rats in each group before and after the operation, and the time it took for the rats to fall from the rotarod was recorded.

#### *2.7.3. Foot misplacement test*

Three days before modelling, the rat was put in the experimental chamber for adaptability testing. The Automatic Foot Misplacement Apparatus (BIO-FMA; Panlab, Barcelona, Spain) with a rat corridor was employed, and the rats walked in the corridor with ladder rungs. The sensors had the capability to detect how many instances a rat's paws slid along the ladder steps. Locotronic software was employed to keep track of the number of steps missed. The rats were positioned at one side of the hallway and were able to move freely along the corridor until they reached the endpoint of sensor measurement at the opposite side, where the entire path of the rats' movement was documented. If the rats changed direction during the recording, walking was repeated until the rats walked through the entire corridor without changing direction. Each rat was recorded three times to obtain the number of steps missed. There were three rats in each group.

### *2.8. In Vitro oxygen glucose deprivation/reoxygenation (OGD/R) and drug treatments*

Cultured hippocampal neurons from mouse embryos were assigned into four groups: sham, model, XNJ and edaravone groups. The cells were incubated for 24 h in the neural basal medium containing 2 % B27 and 2 mL glutamine (Invitrogen, CA, USA), with half of the medium being changed every 48 h. The cells' culture medium was substituted with serum-free and glucose-free Dulbecco's Modified Eagle Medium (DMEM) medium (OGD medium), and cells were cultivated in an anaerobic incubator containing 95 % N2/5 % CO2 mixture for 2 h. After 2 h, the cells were then placed back in a normoxic incubation (95 % air and 5 % CO2) with normal glucose medium for 2 h. The XNJ group was given 1.5 mL/L XNJ injection, and the edaravone group was given 100 μmol/L edaravone injection. On the other hand, the sham and model groups were provided with an equivalent DMEM media after reoxygenation for 24 h. The sham group was treated with OGD medium in normoxic condition and then immediately replaced with normal nerve basal medium.

### *2.9. Flow cytometry in Vitro*

The cells were digested with 0.25 % pancreatin and adjusted to a cell density of approximately $1 \times 10^6$/mL. The suspension (0.2 mL) of cells was transferred from the cell culture plate to a clean tube for centrifugation. After being subjected to centrifugation at a force of 1000 g for a duration of 5 min at ambient temperature, the medium was removed. The pellet of cells was carefully resuspended with 0.2 mL of pre chilled phosphate buffered saline (PBS) solution and centrifuged at 1000 g for 5 min to remove the supernatant. The pellet of cells was softly suspended using 0.2 mL of binding buffer that had been pre-cooled. Then, 5 μL of annexin FITC and 5 μL of PI dye solution were gently added to the mixture. Apoptotic cells were detected using the Annexin V-FITC/PI Apoptosis Detection Kit after being incubated in the dark at room temperature for 15 min. First, cells were washed in PBS. Then, Annexin V-FITC-propidium iodide (P.I.) was used for staining. Next, it was placed in darkness fixed in 70 % ethanol for 1 h. Finally, a flow cytometer was employed to measure the percentage of apoptotic cells.

### *2.10. Flow cytometry in Vivo*

Rats under anesthesia were sacrificed on ice and hippocampal tissue was rapidly removed. Hippocampal tissue was minced adequately in tube and PBS was added to mix well. After being spun at a speed of 500 rpm for a duration of 3 min, the liquid portion was abandoned and pancreatic enzymes were added, which were terminated by adding calf serum after 30 min at 37 °C. after centrifuging at 500 rpm for 3min and discarding the supernatant, PBS was added and the supernatant was obtained. Cell suspension was resuspended in 1x binding buffer. The concentration was adjusted to $1 \times 10^6$/mL. To the flow tube containing 100 mL of cell suspension, 5 mL of Annexin V/FITC solution is introduced, followed by incubation of the mixture at room temperature for 5 min in the absence of light. Propidium iodide solution (10 μL) of 20 μg/mL was added and then 400 μL PBS was added. Flow cytometry was used to examine apoptosis rates.

### *2.11. Electron microscope*

The rats anesthetized and ventilated by precooled PBS (pH7.4) and 2.5 % glutaraldehyde. Subsequently, a tissue block measuring 1 mm on each side was acquired from the adjacent region of the infarct and the corresponding region of rats that underwent a sham operation. The tissue block was placed in a solution of 2.5 % glutaraldehyde at a temperature of 4 °C for a duration of 4 h. Following this, the samples were fixed using a combination of 1 % osmium tetraoxide and 0.1 M phosphate buffer (PB, pH7.4) at room temperature for 2 h. Subsequently, the samples underwent dehydration using a series of graded ethanol solutions and were then embedded in SPI PON 812 epoxy resin at a temperature of 37 °C overnight. Polymerization took place at a temperature of 60° Celsius for a duration of 48 h. The Leica UC7 Ultrathin Cutting Machine was utilized to cut ultra-thin sections (60–80 nm), which were then stained with a mixture of 2 % uranyl acetate and lead citrate for a period of 15 min. Finally, the Phillips CM 100 electron microscope was used for observation.

### 2.12. Measurement of intracellular $Ca^{2+}$ in the hippocampus

A mixture of 50 ppm fluoride was applied to primary neurons for 48 h and washed with PBS afterward. The primary neurons were incubated with fluorescent probe Fluo-4 at 37 °C for 30 min in Fluo-4nw calcium determination reagent and were washed with PBS three times. $Ca^{2+}$ level was assessed by laser scanning confocal microscopy.

### 2.13. Quantitative RT-qPCR analysis

RNA was isolated using TRlzol reagent following the guidelines provided by the manufacturer, and subsequently converted into cDNA using a reverse transcription kit. The steps of the procedure were as follows: denaturation at a temperature of 95 °C for a duration of 10 min, followed by 45 cycles of PCR lasting for 10 s at 95 °C and 30 s at 60 °C. Then, one cycle lasted for 15 s at 95 °C and another cycle lasted for 1 min at 60 °C. Continuous fluorescence measurement was conducted at a temperature of 95 °C for 15 s. Sequence-specific primers for GPR78, CHOP, caspase-12, caspase-9, caspase-3, and GAPDH are shown in Table 1.

### 2.14. Western blot

Tissues samples were lysed in a mixture of protease inhibitors. The whole extraction process was on ice. To assess the protein concentration of tissue samples and cells, a kit for the bicinchoninic acid assay (BCA) protein assay was utilized. By employing 10 % twelve alkyl sulfate polyacrylamide gel electrophoresis, an equivalent quantity of protein was transferred onto the PVDF membrane. Following the sealing of the PVDF membrane using 5 % skim milk powder for 1 h, the membrane was left to incubate with the primary antibody overnight. Primary antibodies include GRP78 (1:1000), CHOP (1:2000), Bcl-2 (1:1000), Bax (1:1000), caspase-12 (1:1000), caspase-9 (1:1000 Abcam), cleaved-caspase-3 (1:1000), GAPDH (1:2000). On the second day, the membrane was incubated with fluorescent labeled secondary antibody (HRP- Goat anti-Rabbit IgG, 1:5000; HRP-Goat anti-Mouse IgG, 1:5000) at room temperature for 1 h. Subsequently, the antibody complex was captured using pierce enhanced chemiluminescence (ECL) western blotting substrate.

### 2.15. Statistical analysis

All statistical analyses were conducted by GraphPad Prism 5 software and SAS 8.2. The data were presented as means ± standard error of means (SEM). These data were checked for normality and homoscedasticity. The Student's *t*-test was utilized to conduct comparisons between two groups. Data test among multiple groups was conducted using One-way analysis of variance (ANOVA). Pairwise comparisons between multiple groups were performed using the LSD method. Non-parametric data were represented by median and the data were analyzed by using Kruskal-Wallis analysis of variance. The $p$ values $< 0.05$ were regarded as statistically significant.

## 3. Results

### 3.1. XNJ improved the neurological outcome and reduced the infarct volume and brain edema in MCAO rats

The infarction rate was assessed using TTC staining. The normal area appeared red, and the infarction area appeared white by TTC staining as shown in Fig. 1A. In the model group, the noticeable infarct region was observed, whereas the XNJ group and edaravone group exhibited a significant decrease in the infarct area, as depicted in Fig. 1B ($p < 0.05$). In addition, neurological deficit score was employed to test whether XNJ could improve neurological function after ischemic stroke. The sham operation group did not show neurological deficits, whereas the model group exhibited noticeable neurological deficits ($p < 0.05$). The neurological deficits were alleviated in both the XNJ and edaravone groups as shown in Fig. 1C. The brain water content was higher in the model group compared to the sham operation group, while the brain water content in the XNJ group and edaravone group were lower than those in the model

**Table 1**
Sequence-specific primers for GPR78, CHOP, caspase-12, caspase-9, caspase-3 and GAPDH.

| Gene primer | Sequence |
|---|---|
| *Chop-F* | *5′-TGTTGAAGATGAGCGGGTGG-3′* |
| *Chop-R* | *5′-CGATGGTGCTGGGTACACTT-3′* |
| *GAPDH -F* | *5′-GGGTCCCAGCTTAGGTTCAT-3′* |
| *GAPDH-R* | *5′-CTCGTGGTTCACACCCATCA-3′* |
| *Caspase3-F* | *5′-GCTTGGAACGGTACGCTAAG-3′* |
| *Caspase3-R* | *5′-AGCCTCCACCGGTATCTTCT-3′* |
| *Caspase12-F* | *5′-ATCCAACGGTGTTCTGGTCC-3′* |
| *Caspase12-R* | *5′-TCTCGCATCCCCAAAAGGTC-3′* |
| *Caspase9-F* | *5′-CACCTTCCCAGGTTGCCAAT-3′* |
| *Caspase9 -R* | *5′-CATCCATTGCACTCCGGTCT-3′* |
| *GRP78 -F* | *5′-GTGTGTGAGACCAGAACCGT-3′* |
| *GRP78 -R* | *5′-TCGCTGGGCATCATTGAAGT-3′* |

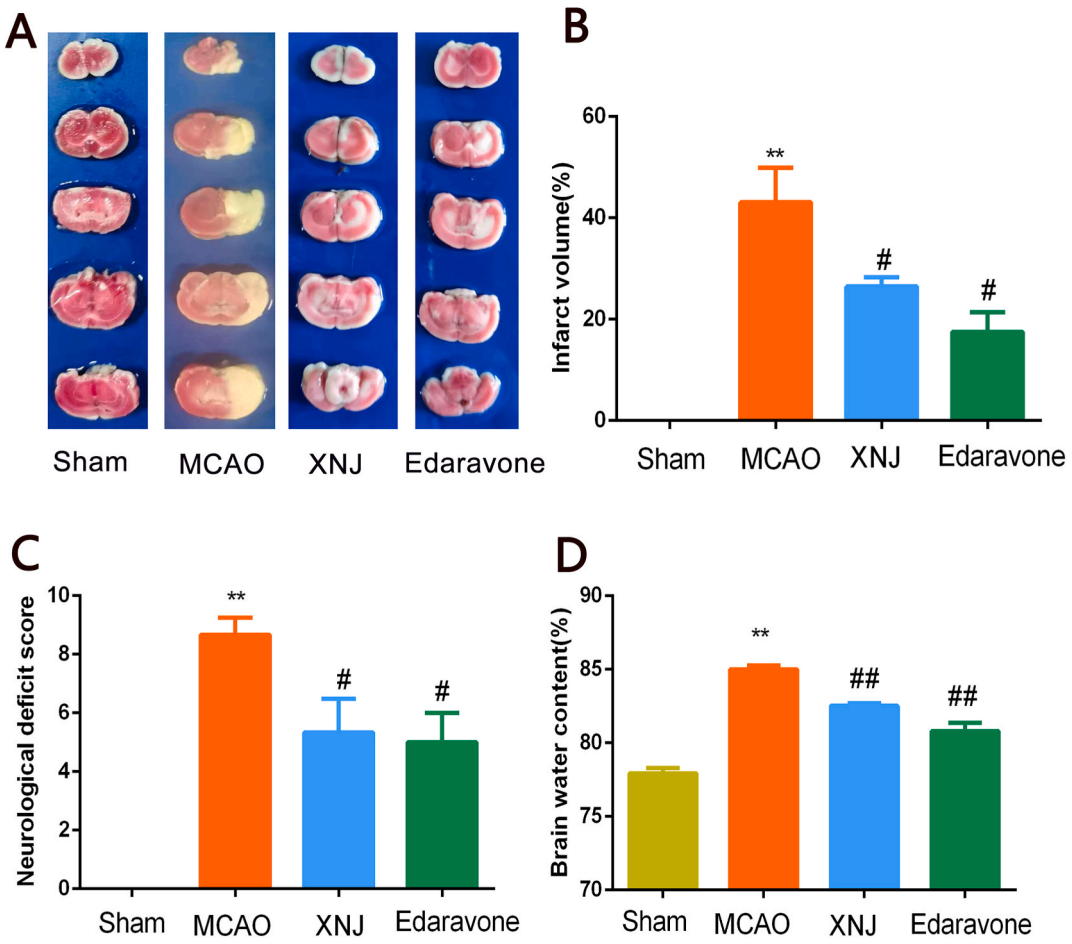


**Fig. 1.** XingNaoJing (XNJ) injection relieves cerebral ischemia reperfusion injury and brain edema. (A) Representative pictures of TTC staining. (B) Quantitative analysis of infarct volumes. (C) Effects of XNJ on neurological deficits score evaluated by the modified neurological severity score (mNSS). (D) Effects of XNJ on brain edema evaluated by the brain water content. Data are presented as means ± SEM. *$p < 0.05$, **$p < 0.01$ vs. sham group; #$p < 0.05$, ##$p < 0.01$ vs. MCAO group.

group ($p < 0.05$), indicating that the edema was reduced after XNJ and edaravone treatment, as shown in Fig. 1D.

### 3.2. XNJ improved motor behavioral performance in MCAO rats

Grip strength test, rotarod and foot misplacement tests were adopted to assess whether XNJ improved the motor performance in MCAO rats. In comparison with the sham operation group, the rats in the MCAO group had worse grip and shorter time in rotarod and the rats significantly performed more missteps ($p < 0.05$). When XNJ injection and edaravone were respectively injected into the MCAO rat, the rats in the XNJ group and edaravone group exhibited notable enhancements in grip strength and movement time on rotarod ($p < 0.05$), and the number of missteps was also reduced ($p < 0.05$). In detail, for treatment of XNJ, there was a significant reduction in both front leg errors and tail errors compared to the model group ($p < 0.05$). Results of all motor performance assessments for all groups tested are showed in Fig. 2A–D.

### 3.3. XNJ suppressed cell apoptosis and reduced the neuron-structural damage of cerebral ischemia-reperfusion

To evaluate the potential neuroprotective effect of XNJ, transmission electron microscopy was applied to examine neuronal ultrastructure. The cortical neurons in the sham group exhibited distinct boundaries, characterized by sizable and circular nuclei, consistent chromatin, and transparent cytoplasm. In the model group, cortical neurons showed pyknotic and condensed chromatin in the nucleus and dissolved cytoplasm with vacuolization around the periphery. Compared with the model group, neuron-structural damages in XNJ group and edaravone group were alleviated, and the morphology of neurons was complete but irregular as shown in Fig. 3A. The results demonstrated that XNJ could reduce the ultrastructure damage of neurons in MCAO rats. In order to assess the impact of XNJ on cell apoptosis, the apoptosis rate of neurons in the hippocampus of the MCAO rats was detected by flow cytometry.

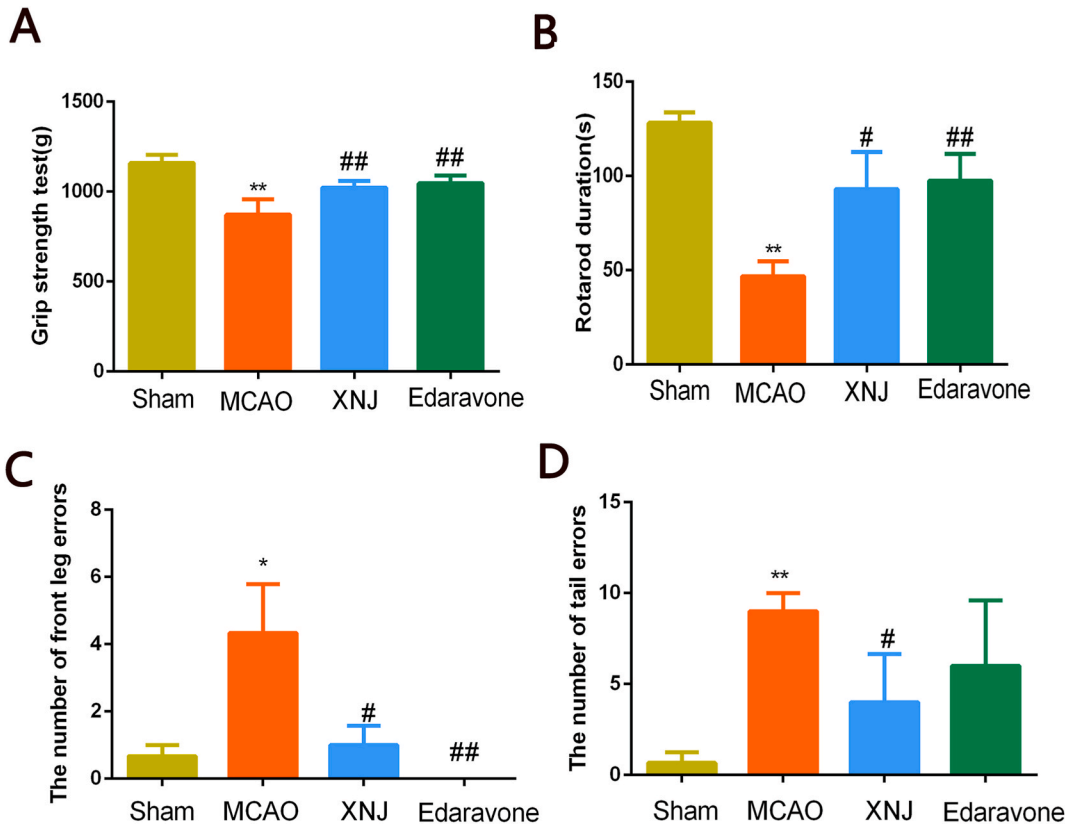


**Fig. 2.** XNJ improves the motor performance. (A) The effect of XNJ on grip strength test. (B) Rotarod duration. (C) The front leg errors. (D) The tail errors. Data are presented as means ± SEM. $*p < 0.05$, $**p < 0.01$ vs. sham group; $\#p < 0.05$, $\#\#p < 0.01$ vs. MCAO group.

The apoptosis rate in sham group was low, while the apoptosis rate in model group markedly increased in comparison with sham group as shown in Fig. 3B. After XNJ and edaravone treatment, the apoptosis rate of the XNJ and edaravone group reduced markedly ($p < 0.05$) as shown in Fig. 3C.

### *3.4. XNJ suppressed OGD/R-induced apoptosis and reduced calcium release*

To evaluate the anti-apoptosis effect of XNJ in cultured neurons, flow cytometry was conducted to calculate the apoptosis rate. The sham group had a low level of apoptosis, and a significant larger amount of apoptosis was observed after OGD/R. The apoptosis rates of the XNJ group and edaravone group were lower compared to the model group, as depicted in Fig. 4A. The results suggested that XNJ had a certain anti-apoptosis effect. Additionally, to explore the influence of XNJ on $Ca^{2+}$ content, the level of intracellular $Ca^{2+}$ content was determined by laser confocal. The fluorescence intensity of $Ca^{2+}$ was markedly higher in the model group than that observed in the sham operation group. However, in contrast to the model group, the administration of XNJ injection and edaravone significantly decreased calcium release indicated by lower green fluorescence intensity as shown in Fig. 4B and C.

### *3.5. XNJ alleviates apoptosis of neurons after I/R and OGD/R-induced apoptosis via ERS inhibition*

To further examine the mechanism that whether the anti-apoptotic impact of XNJ was associated with XNJ. The key molecules of ERS, including GRP78, CHOP, Bcl-2, Bax, caspase-12, caspase-9 and cleaved-caspase-3 mediated apoptosis pathway was assessed by western blot and RT-PCR. In the western blot experiment, the expression of GRP78, CHOP, Bax, caspase-12, caspase-9 and cleaved-caspase-3 were markedly upregulated in the MCAO model group as compared to the sham group. However, the application of XNJ injection and edaravone could significantly reverse the expression of CHOP, GRP78, Bax, caspase-12, caspase-9 and cleaved-caspase-3 as shown in Fig. 5A and B. In the model group, the Bcl-2/Bax ratio was comparatively lower compared to the sham group. The application of XNJ injection and edaravone could increase the ratio of Bcl-2/Bax. In the RT-PCR experiment, the MCAO model group exhibited increased expression of GRP78 mRNA, caspase-12 mRNA, caspase-9 mRNA, pro-caspase-3 mRNA, and CHOP mRNA in comparison to the sham group. However, these changes were reversed by XNJ injection and edaravone treatment as shown in Fig. 6A. These results suggested that XNJ could protect rats against apoptosis after I/R via inhibiting the RES pathway.We further tested the effects of XNJ on OGD/R-induced apoptosis by RT-PCR. As indicated in Fig. 5B, the expressions of GRP78 mRNA, CHOP mRNA,

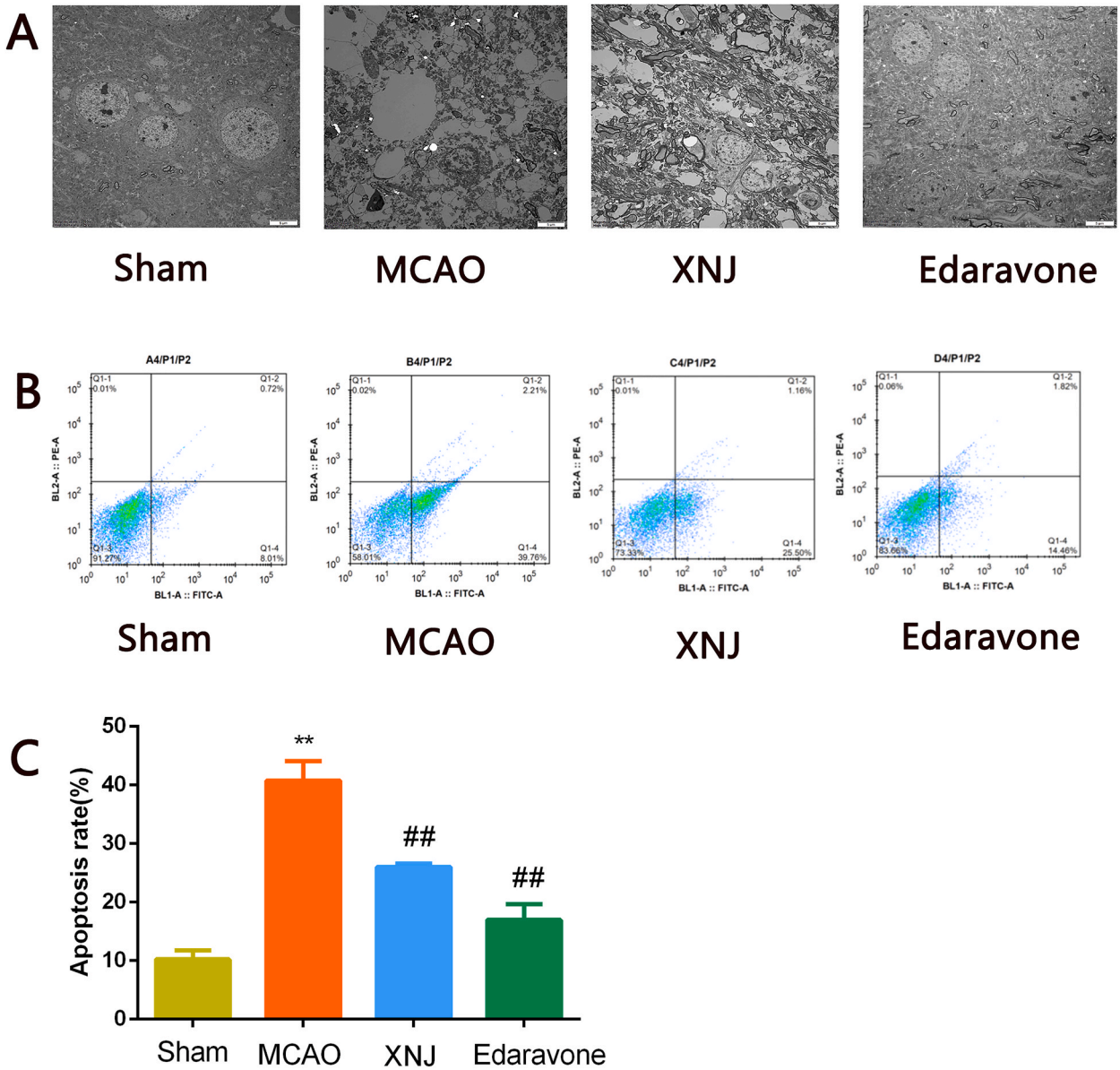


**Fig. 3.** XNJ reduces cell structure damage and inhibits cell apoptosis. (A) the effect of XNJ reducing structural damage observed by Electron microscope. (B) Representative pictures of apoptosis detection in MCAO rats. (C) Quantitative analysis of apoptosis in MCAO rats. Data are presented as means ± SEM. $*p < 0.05$, $**p < 0.01$ vs. sham group; $\#p < 0.05$, $\#\#p < 0.01$ vs. MCAO group.

caspase-12 mRNA, caspase-9 mRNA, and caspase-3 mRNA in OGD/R-treated hippocampus cells were higher than that in sham group. However, these mRNA were decreased in the XNJ and edaravone groups as shown Fig. 6B. These experiments data indicated that XNJ could alleviate OGD/R-induced injury in hippocampus cells via inhibiting the ERS pathway.

## 4. Discussion

The etiology of cerebral vascular disease is characterized by a multifaceted pathological process, encompassing various mechanisms such as blood-brain barrier disruption, inflammation, apoptosis, and oxidative stress [9,32,33]. In the context of treating ischemic stroke and enhancing neurological function, aside from interventional thrombectomy and thrombolysis, there is currently a lack of FDA-approved drugs that have demonstrated efficacy [34]. Previous investigations into neuroprotective agents have yielded unfavorable outcomes, partly due to the limited effectiveness of single-target compounds in addressing multiple-target diseases and mechanisms [35,36]. However, Traditional Chinese Medicine (TCM) exhibits the attributes of multi-target and multi-mechanism intervention for the treatment of diseases [37,38]. Previous meta-analysis has demonstrated the efficacy of the Chinese patent

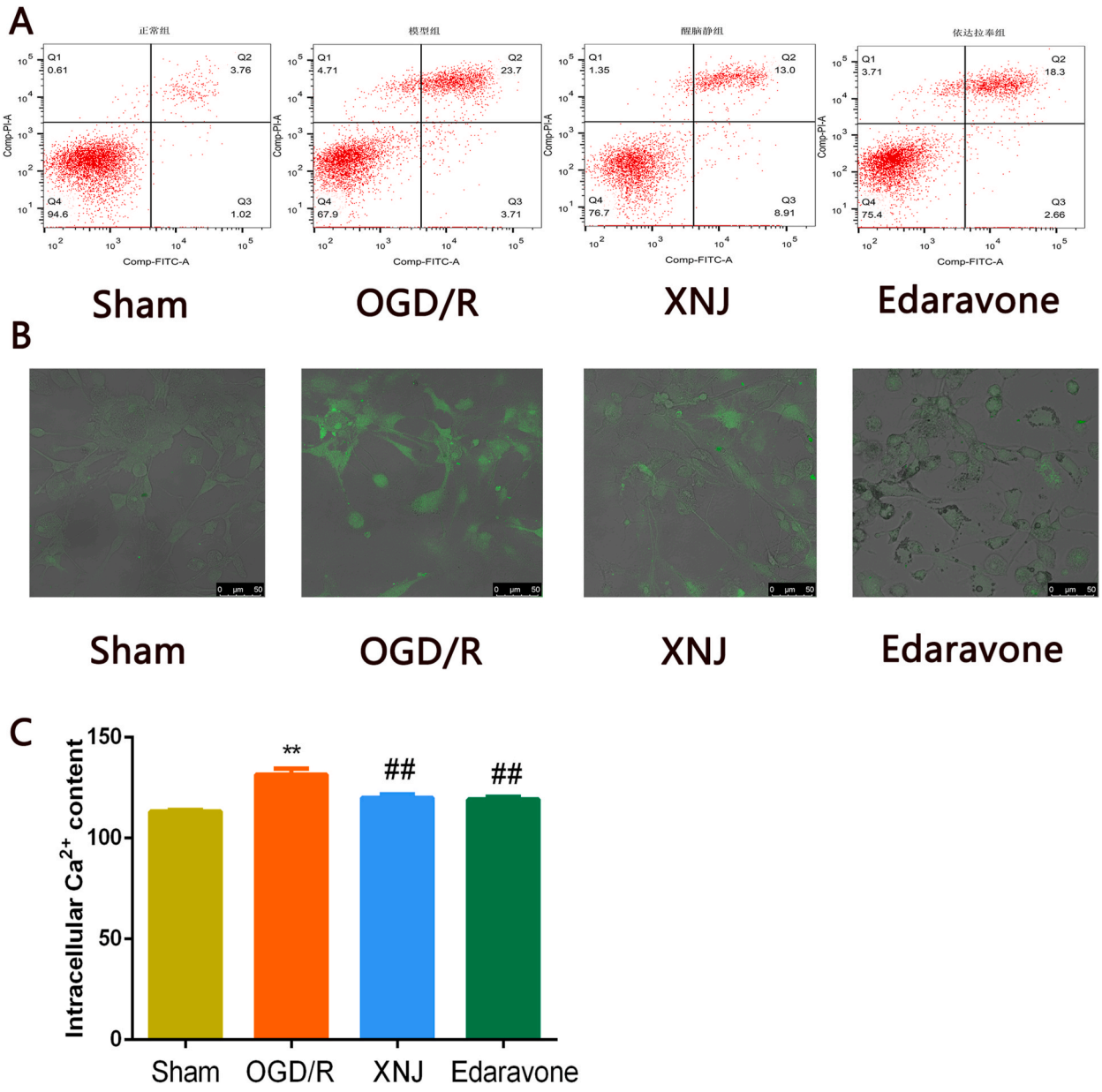


**Fig. 4.** XNJ suppresses OGD/R-induced apoptosis and reduces intracellular $Ca^{2+}$ content in the hippocampus. (A) Representative pictures of apoptosis detection in OGD/R cell model. (B) Representative pictures of $Ca^{2+}$ content detected by confocal laser scanning. (C) Quantitative analysis of $Ca^{2+}$ content. Data are presented as means ± SEM. $*p < 0.05$, $**p < 0.01$ vs. sham group; $\#p < 0.05$, $\#\#p < 0.01$ vs. OGD/R group.

medicine—XNJ injection in ameliorating neurological deficits caused by ischemic stroke [39]. Several earlier investigations have indicated that XNJ has the potential to enhance neurological function recovery by suppressing NOD-like receptor thermal protein domain associated protein 3 (NLRP3) inflammasomes [28]. Nevertheless, the underlying mechanism of XNJ in the management of ischemic stroke is still not fully revealed.

Cerebral ischemia reperfusion initiates a cascade reaction in the brain, ultimately resulting in programmed cell death and necrosis through multiple mechanisms and pathways [40]. Previous studies have demonstrated that XNJ has the ability to mitigate cell apoptosis by regulating ferroptosis and PI3K/Akt-mediated eNOS Phosphorylation [27,41]. Moreover, ERS also has a crucial function in the occurrence of neuronal death caused by ischemia and reperfusion [42]. It is unclear whether XNJ could perform the anti-apoptotic effect through regulating ERS.

Recent studies revealed that reducing ischemia-induced ERS can protect neurons from ischemia-reperfusion injury [43,44]. In our present study, we have provided evidence that XNJ effectively attenuates neuronal cell death induced by ERS in MCAO rats and OGD/R neurons. The endoplasmic reticulum, as a significant subcellular organ, is accountable for the correct folding and classification

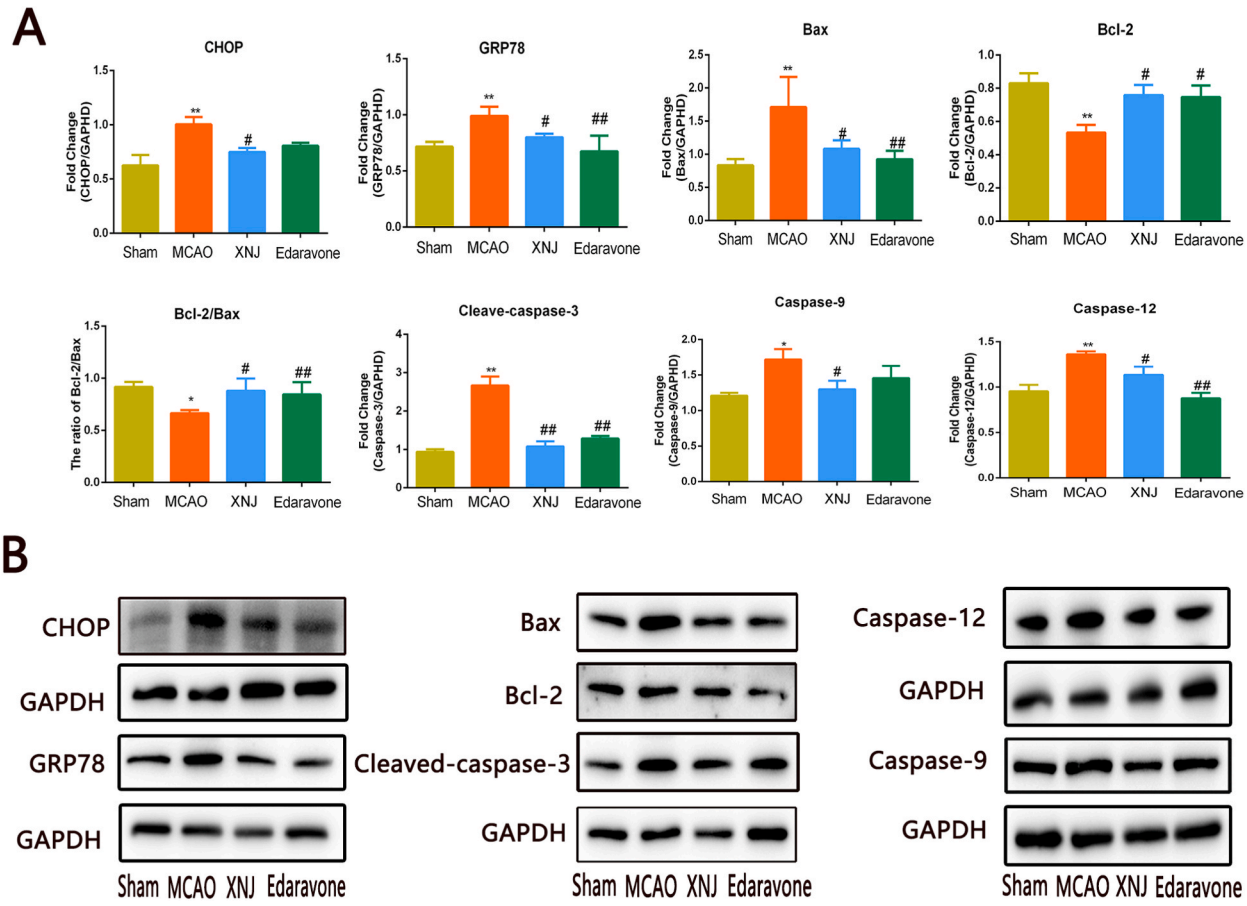


**Fig. 5.** XNJ regulates related proteins of ERS. (A) Quantitative analysis of CHOP, GRP78, Bax, Bcl-2, cleaved-caspase-3, caspase-9 and caspase-12 in western blot. (B) Representative western blot analysis of CHOP, GRP78, Bax, Bcl-2, cleaved-caspase-3, caspase-9 and caspase-12. Data are presented as means ± SEM. $*p < 0.05$, $**p < 0.01$ vs. sham group; $\#p < 0.05$, $\#\#p < 0.01$ vs. MCAO group.

of proteins [45]. Reperfusion following ischemia results in a state of cellular stress, marked by a lack of glucose, depletion of calcium in the endoplasmic reticulum, and exposure to free radicals. As a result, unfolded proteins accumulate in the endoplasmic reticulum's lumen. In response, an unfolded protein response is initiated to restore endoplasmic reticulum function by activating transmembrane receptors, within the endoplasmic reticulum, such as PERK, inositol-requiring enzymes, and activating transcription factor 6 [46]. Phosphorylation of eukaryotic translation initiation factor 2 occurs upon PERK activation, resulting in enhanced translation of activated transcription factor 4 (ATF4) and CHOP. The activated CHOP plays a key role in ERS-induced apoptosis by down-regulating the anti-apoptotic factor Bcl-2 [47,48].

To access the impact of XNJ on ischemic stroke, edaravone was selected as a positive control due to its neuroprotective properties against free radicals, which have been demonstrated in animal models [49]. Li C et al. found that edaravone could inhibit cell apoptosis [50]. Ren C et al. determine that edaravone could reduce infarct size and brain edema, and rehabilitate neurological function [51]. TTC staining, brain water content assessment, and mNSS were utilized to assess the impact of XNJ. Motor performance was evaluated through grip strength, rotarod, and foot misplacement tests to examine the effect of XNJ. Similar to edaravone, XNJ exhibited a comparable protective effect. Our findings demonstrate that XNJ exerts neuroprotective effects by enhancing neuronal survival, reducing infarct size, and alleviating brain edema in rats subjected to ischemia-reperfusion. Furthermore, XNJ treatment significantly restored the neurological function of MCAO rats.

In terms of motor performance, XNJ exhibited a notable enhancement in the forelimb grip of rats subjected to MCAO. Additionally, XNJ demonstrated a significant improvement in the rats' endurance on the wheel, resulting in an increased running time. Moreover, XNJ effectively reduced the overall count of incorrect steps in rats, particularly in the forelimb and hindlimb, although its positive impact on the tail was comparatively less pronounced. This observation may be attributed to XNJ's ability to mitigate neuronal apoptosis within the jurisdiction area of the middle cerebral artery.

Based on flow cytometry, it was also shown that XNJ significantly increased the number of neurons that survived, and transmission electron microscopy showed that XNJ could protect neurons by reducing the structural damage. By flow cytometry, it was also observed that XNJ reduced cell apoptosis in cultured mouse hippocampal cells in the OGD/R model. In addition, the utilization of RT-PCR and western blot demonstrated that treatment with XNJ exhibited significant down-regulation of GRP78, CHOP, Bax, caspase-12,

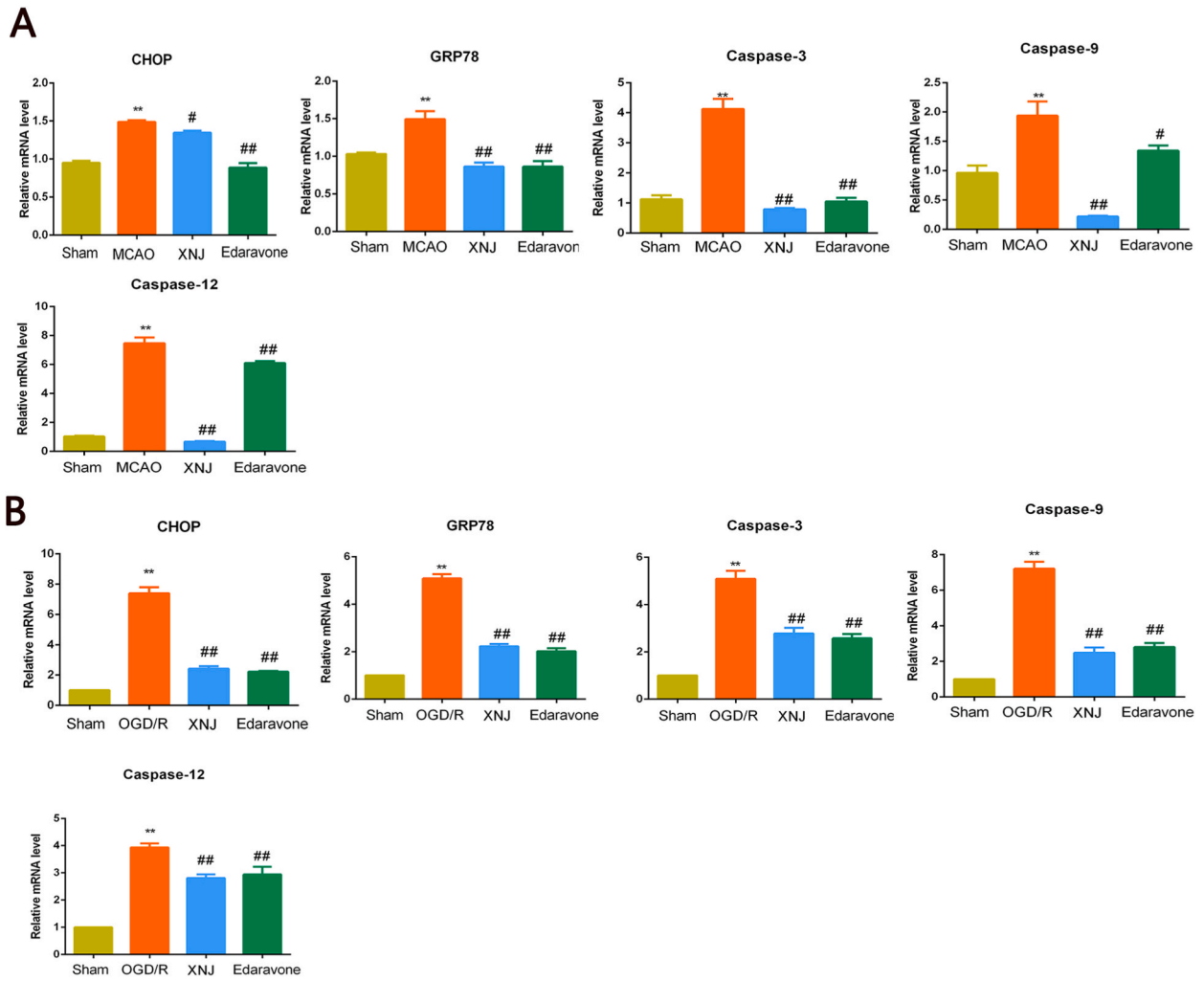


**Fig. 6.** XNJ regulates related mRNA levels of ERS. (A) The mRNA levels of CHOP, GRP78, caspase-3, caspase-9 and caspase-12 in cerebral cortex infarct area of MCAO rats. (B) The mRNA levels of CHOP, GRP78, caspase-3, caspase-9 and caspase-12 in cultured neurons. The cell experiment was repeated 3 times independently. Data are presented as means ± SEM. $*p < 0.05$, $**p < 0.01$ vs. sham group; $\#p < 0.05$, $\#\#p < 0.01$ vs. MCAO group.

caspase-9, and cleaved-caspase-3 expressions in the cortical tissue of MCAO model. Simultaneously, XNJ up-regulated the expression of nerve protective protein Bcl-2. In cultured neurons after ischemia-reperfusion, the expressions of GRP78, CHOP, caspase-12, caspase-9 and cleaved-caspase-3 were decreased by XNJ. These results showed that XNJ protected neuronal cells from ischemia-reperfusion injury by reducing ERS-induced apoptosis.

In addition, calcium overload is a part of the pathogenesis of ischemic stroke and an integral part of ERS [52,53]. In relation to ischaemic brain, an excess of calcium is induced, resulting in $Ca^{2+}$ release from the endoplasmic reticulum via calcium-dependent protease calpain, which specifically targets calcium regulatory proteins. Prolonged depletion of $Ca^{2+}$ within the endoplasmic reticulum hinders proper protein processing, leading to an imbalance in the endoplasmic reticulum homeostasis and an increase in unfolded proteins. Consequently, these processes contribute to the promotion and exacerbation of ERS, ultimately triggering apoptosis of ischemic neurons [54]. In this study, the concentration of $Ca^{2+}$ in the hippocampus was examined by laser confocal microscopy. The study revealed that XNJ has the capability to decrease the concentration of $Ca^{2+}$ in the hippocampus, suggesting its potential in mitigating ERS through the reduction of calcium overload.

One of the limitations of the study is the lack of investigation into the optimal administration time. Given the criticality of time for ischemic stroke patients, previous research has demonstrated a significant rise in mortality rates within the ischemic penumbra with each passing hour, emphasizing the importance of early intervention. In theory, the preservation of a greater number of neurons and the subsequent improvement in patient prognosis are directly proportional to the early administration of treatment. For this particular study, an administration time of 2 h after the establishment of MCAO in rats was chosen, although its optimality remains uncertain. Consequently, it is imperative to conduct experiments in future research endeavors to determine the most suitable administration time.

## 5. Conclusion

We found that XNJ not only reduced brain edema, infarct volume and improved motor performance, but also suppressed cell apoptosis caused by cerebral ischemia-reperfusion injury. We identified ERS was involved in regulating cell apoptosis and XNJ could inhibit ERS to reduce apoptosis rate by detecting the expression of relative proteins. Overall, our data suggest that XNJ may be an effective treatment to acute ischemic stroke.

## Ethics statement

The present study was allowed by the Animal Ethics Committee of Dongzhimen Hospital affiliated with Beijing University of Chinese Medicine (registration and ethical approval number: 20–42 approved on November 20, 2020).

## Data availability statement

Data are available from the corresponding author and the first author on reasonable request.

## Funding statement

This research was funded by the Beijing University of Chinese Medicine Project [2019-JYB-JS-034], Clinical Cooperation Capacity Building Project of Traditional Chinese and Western Medicine for Major and Difficult Diseases [YW082]. Construction Project of Beijing Traditional Chinese Medicine Cerebrovascular Disease Prevention and Treatment Office of Beijing Municipal Administration of Traditional Chinese Medicine [YW083].

## CRediT authorship contribution statement

**Xinglu Dong:** Writing – review & editing, Writing – original draft, Methodology, Funding acquisition. **Chuanpeng Li:** Writing – review & editing, Writing – original draft, Methodology, Data curation. **Yaoyao Yao:** Data curation. **Fengzhi Liu:** Data curation. **Ping Jiang:** Data curation. **Ying Gao:** Project administration, Funding acquisition.

## Declaration of competing interest

The authors declare that they have no known competing financial interests or personal relationships that could have appeared to influence the work reported in this paper.

## Acknowledgements

Declared none.

## Appendix A. Supplementary data

Supplementary data to this article can be found online at https://doi.org/10.1016/j.heliyon.2024.e25267.

## References

[1] Y.J. Wang, Z.X. Li, H.Q. Gu, Y. Zhai, Y. Jiang, X.Q. Zhao, et al., China stroke Statistics 2019: a report from the National center for Healthcare quality management in neurological diseases, China National clinical research center for neurological diseases, the Chinese stroke association, National center for Chronic and Non-communicable disease control and Prevention, Chinese center for disease control and Prevention and Institute for global neuroscience and stroke collaborations, Stroke Vasc Neurol 5 (3) (2020) 211–239, https://doi.org/10.1136/svn-2020-000457.

[2] Tsao, Heart disease and stroke statistics-2022 update: a report from the American Heart association, Circulation 146 (10) (2022) E141, https://doi.org/10.1161/Cir.0000000000001074. E141.

[3] J. Xu, X. Zhang, A.M. Jin, Y.S. Pan, Z.X. Li, X. Meng, et al., Trends and risk factors associated with stroke recurrence in China, 2007-2018, JAMA Netw. Open 5 (6) (2022) e2216341, https://doi.org/10.1001/jamanetworkopen.2022.16341.

[4] W.J. Powers, A.A. Rabinstein, T. Ackerson, O.M. Adeoye, N.C. Bambakidis, K. Becker, et al., Guidelines for the early management of patients with acute ischemic stroke: 2019 update to the 2018 guidelines for the early management of acute ischemic stroke: a guideline for healthcare professionals from the American heart association/American stroke association, Stroke 50 (12) (2019) e344–e418, https://doi.org/10.1161/STR.0000000000000211.

[5] Q.Z. Tuo, S.T. Zhang, P. Lei, Mechanisms of neuronal cell death in ischemic stroke and their therapeutic implications, Med. Res. Rev. 42 (1) (2022) 259–305, https://doi.org/10.1002/med.21817.

[6] A. Jurcau, A. Simion, Neuroinflammation in cerebral ischemia and ischemia/reperfusion injuries: from pathophysiology to therapeutic strategies, Int. J. Mol. Sci. 23 (1) (2022) 14, https://doi.org/10.3390/ijms23010014.

[7] M. Barzegar, G. Kaur, F.N.E. Gavins, Y. Wang, C.J. Boyer, J.S. Alexander, Potential therapeutic roles of stem cells in ischemia-reperfusion injury, Stem Cell Res. 37 (2019) 101421, https://doi.org/10.1016/j.scr.2019.101421.

[8] Y. Zhang, D.B. Cheng, C.X. Jie, T. Liu, S.X. Huang, S.J. Hu, Leptin alleviates endoplasmic reticulum stress induced by cerebral ischemia/reperfusion injury via the PI3K/Akt signaling pathway, Biosci. Rep. 42 (12) (2022) BSR20221443, https://doi.org/10.1042/Bsr20221443.

[9] L. Wu, X. Xiong, X. Wu, Y. Ye, Z. Jian, Z. Zhi, et al., Targeting oxidative stress and inflammation to prevent ischemia-reperfusion injury, Front. Mol. Neurosci. 13 (2020) 28, https://doi.org/10.3389/fnmol.2020.00028.

[10] G. Enzmann, S. Kargaran, B. Engelhardt, Ischemia-reperfusion injury in stroke: impact of the brain barriers and brain immune privilege on neutrophil function, Ther Adv Neurol Disord 11 (2018) 1756286418794184, https://doi.org/10.1177/1756286418794184.

[11] J. Li, T. Tao, J. Xu, Z. Liu, Z.H. Zou, M.L. Jin, HIF-1α attenuates neuronal apoptosis by upregulating EPO expression following cerebral ischemia-reperfusion injury in a rat MCAO model, Int. J. Mol. Med. 45 (4) (2020) 1027–1036, https://doi.org/10.3892/ijmm.2020.4480.

[12] A.B. Uzdensky, Apoptosis regulation in the penumbra after ischemic stroke: expression of pro- and antiapoptotic proteins, Apoptosis 24 (9–10) (2019) 687–702, https://doi.org/10.1007/s10495-019-01556-6.

[13] F.J. Bock, S.W.G. Tait, Mitochondria as multifaceted regulators of cell death, Nat. Rev. Mol. Cell Biol. 21 (2) (2020) 85–100, https://doi.org/10.1038/s41580-019-0173-8.

[14] M. Lam, S.A. Marsters, A. Ashkenazi, P. Walter, Misfolded proteins bind and activate death receptor 5 to trigger apoptosis during unresolved endoplasmic reticulum stress, Elife 9 (2020) e52291, https://doi.org/10.7554/eLife.52291.

[15] H. Hu, M. Tian, C. Ding, S. Yu, The C/EBP homologous protein (CHOP) transcription factor functions in endoplasmic reticulum stress-induced apoptosis and microbial infection, Front. Immunol. 9 (2018) 3083, https://doi.org/10.3389/fimmu.2018.03083.

[16] A. Almanza, A. Carlesso, C. Chintha, S. Creedican, D. Doultsinos, B. Leuzzi, et al., Endoplasmic reticulum stress signalling - from basic mechanisms to clinical applications, FEBS J. 286 (2) (2019) 241–278, https://doi.org/10.1111/febs.14608.

[17] R.L. Wiseman, J.S. Mesgarzadeh, L.M. Hendershot, Reshaping endoplasmic reticulum quality control through the unfolded protein response, Mol. Cell 82 (8) (2022) 1477–1491, https://doi.org/10.1016/j.molcel.2022.03.025.

[18] H. Chino, N. Mizushima, Er-Phagy, Quality control and Turnover of endoplasmic reticulum, Trends Cell Biol. 30 (5) (2020) 384–398, https://doi.org/10.1016/j.tcb.2020.02.001.

[19] I.L. Lemmer, N. Willemsen, N. Hilal, A. Bartelt, A guide to understanding endoplasmic reticulum stress in metabolic disorders, Mol. Metabol. 47 (2021) 101169, https://doi.org/10.1016/j.molmet.2021.101169.

[20] S.V.S. Rana, Endoplasmic reticulum stress induced by toxic elements-a review of recent developments, Biol. Trace Elem. Res. 196 (1) (2020) 10–19, https://doi.org/10.1007/s12011-019-01903-3.

[21] L.H. Xu, Y.L. Bi, Y.Z. Xu, Y.H. Wu, X.X. Du, Y.X. Mou, et al., Suppression of CHOP reduces neuronal apoptosis and rescues cognitive impairment induced by intermittent hypoxia by inhibiting Bax and Bak activation, Neural Plast. 2021 (2021) 4090441, https://doi.org/10.1155/2021/4090441.

[22] Y.P. Chung, C.C. Yen, F.C. Tang, K.I. Lee, S.H. Liu, C.C. Wu, et al., Methylmercury exposure induces ROS/Akt inactivation-triggered endoplasmic reticulum stress-regulated neuronal cell apoptosis, Toxicology 425 (2019) 152245, https://doi.org/10.1016/j.tox.2019.152245.

[23] T. Zhang, C. Wu, X. Yang, Y. Liu, H. Yang, L. Yuan, et al., Pseudoginsenoside-F11 protects against Transient cerebral ischemia injury in rats involving Repressing calcium overload, Neuroscience 411 (2019) 86–104, https://doi.org/10.1016/j.neuroscience.2019.05.030.

[24] W. Zhang, F. Ye, N. Pang, M. Kessi, J. Xiong, S. Chen, et al., Restoration of Sarco/endoplasmic reticulum $Ca^{2+}$-ATPase activity functions as a pivotal therapeutic target of anti-Glutamate-induced Excitotoxicity to attenuate endoplasmic reticulum $Ca^{2+}$ depletion, Front. Pharmacol. 13 (2022) 877175, https://doi.org/10.3389/fphar.2022.877175.

[25] Y. Guo, S. Yan, L. Xu, G. Zhu, X. Yu, X. Tong, Use of angong niuhuang in treating central nervous system diseases and related research, Evid Based Complement Alternat Med 2014 (2014) 346918, https://doi.org/10.1155/2014/346918.

[26] B. Wu, M. Liu, H. Liu, W. Li, S. Tan, S. Zhang, et al., Meta-analysis of traditional Chinese patent medicine for ischemic stroke, Stroke 38 (6) (2007) 1973–1979, https://doi.org/10.1161/STROKEAHA.106.473165.

[27] Y.M. Zhang, X.Y. Qu, J.H. Zhai, L.N. Tao, H. Gao, Y.Q. Song, et al., Xingnaojing injection protects against cerebral ischemia reperfusion injury via PI3K/Akt-Mediated eNOS Phosphorylation, Evid Based Complement Alternat Med 2018 (2018) 2361046, https://doi.org/10.1155/2018/2361046.

[28] X.Y. Qu, Y.M. Zhang, L.N. Tao, H. Gao, J.H. Zhai, J.M. Sun, et al., XingNaoJing injections protect against cerebral ischemia/reperfusion injury and alleviate blood-brain barrier disruption in rats, through an underlying mechanism of NLRP3 inflammasomes suppression, Chin. J. Nat. Med. 17 (7) (2019) 498–505, https://doi.org/10.1016/S1875-5364(19)30071-8.

[29] Xf Tan, T. Qin, N. Li, Yg Yang, Jh Zheng, L. Xie, et al., High-potassium preconditioning enhances tolerance to focal cerebral ischemia-reperfusion injury through anti-apoptotic effects in male rats, J. Neurosci. Res. 97 (10) (2019) 1253–1265, https://doi.org/10.1002/jnr.24483.

[30] L. Li, J.-Q. Si, Z.-W. Han, Y.-C. Chang, Y. Zhou, H. Zhang, et al., GPER agonist G1 suppresses neuronal apoptosis mediated by endoplasmic reticulum stress after cerebral ischemia/reperfusion injury, Neural Regeneration Research 14 (7) (2019) 1221–1229, https://doi.org/10.4103/1673-5374.251571.

[31] S. Ma, X. Liu, B. Cheng, Z. Jia, H. Hua, Y. Xin, Chemical characterization of polysaccharides isolated from scrophularia ningpoensis and its protective effect on the cerebral ischemia/reperfusin injury in rat model, Int. J. Biol. Macromol. 139 (2019) 955–966, https://doi.org/10.1016/j.ijbiomac.2019.08.040.

[32] F. Sivandzade, S. Prasad, A. Bhalerao, L. Cucullo, NRF2 and NF-B interplay in cerebrovascular and neurodegenerative disorders: Molecular mechanisms and possible therapeutic approaches, Redox Biol. 21 (2019) 101059, https://doi.org/10.1016/j.redox.2018.11.017.

[33] X. Hu, T.M. De Silva, J. Chen, F.M. Faraci, Cerebral vascular disease and Neurovascular injury in ischemic stroke, Circ. Res. 120 (3) (2017) 449–471, https://doi.org/10.1161/CIRCRESAHA.116.308427.

[34] G. Duloquin, M. Graber, L. Baptiste, S. Mohr, L. Garnier, M. Ndiaye, et al., Management of ischemic stroke in the acute phase, Revue De Medecine Interne 43 (5) (2022) 286–292, https://doi.org/10.1016/j.revmed.2021.08.003.

[35] S. Paul, E. Candelario-Jalil, Emerging neuroprotective strategies for the treatment of ischemic stroke: an overview of clinical and preclinical studies, Exp. Neurol. 335 (2021) 113518, https://doi.org/10.1016/j.expneurol.2020.113518.

[36] X.Y. Xiong, L. Liu, Q.W. Yang, Refocusing neuroprotection in cerebral reperfusion Era: New Challenges and strategies, Front. Neurol. 9 (2018) 249, https://doi.org/10.3389/fneur.2018.00249.

[37] L. Ren, X. Zheng, J. Liu, W. Li, W. Fu, Q. Tang, et al., Network pharmacology study of traditional Chinese medicines for stroke treatment and effective constituents screening, J. Ethnopharmacol. 242 (2019) 112044, https://doi.org/10.1016/j.jep.2019.112044.

[38] T. Zhu, L. Wang, Y.C. Feng, G.B. Sun, X.B. Sun, Classical active ingredients and extracts of Chinese Herbal medicines: Pharmacokinetics, Pharmacodynamics, and molecular mechanisms for ischemic stroke, Oxid. Med. Cell. Longev. 2021 (2021) 8868941, https://doi.org/10.1155/2021/8868941.

[39] Z.Y. Tian, L.D. Feng, Y. Xie, D.H. Xu, C.Y. Zhang, L.B. Kong, et al., Chinese Herbal medicine Xingnaojing injection for acute ischemic stroke: an overview of Systematic reviews and meta-analyses, Front. Pharmacol. 12 (2021) 659408, https://doi.org/10.3389/fphar.2021.659408.

[40] A. Datta, D. Sarmah, L. Mounica, H. Kaur, R. Kesharwani, G. Verma, et al., Cell death pathways in ischemic stroke and targeted pharmacotherapy, Transl Stroke Res 11 (6) (2020) 1185–1202, https://doi.org/10.1007/s12975-020-00806-z.

[41] H. Liu, N. An, L. Wang, Y. Li, K. Song, Y. Sun, et al., Protective effect of Xingnaojing injection on ferroptosis after cerebral ischemia injury in MCAO rats and SH-SY5Y cells, J. Ethnopharmacol. 301 (2023) 115836, https://doi.org/10.1016/j.jep.2022.115836.

[42] L.M. Chi, D. Jiao, G.X. Nan, H.H. Yuan, J. Shen, Y. Gao, miR-9-5p attenuates ischemic stroke through targeting ERMP1-mediated endoplasmic reticulum stress, Acta Histochem. 121 (8) (2019) 151438, https://doi.org/10.1016/j.acthis.2019.08.005.

[43] F. Wu, J. Qiu, Y. Fan, Q. Zhang, B. Cheng, Y. Wu, et al., Apelin-13 attenuates ER stress-mediated neuronal apoptosis by activating Galphai/Galphaq-CK2 signaling in ischemic stroke, Exp. Neurol. 302 (2018) 136–144, https://doi.org/10.1016/j.expneurol.2018.01.006.

[44] Y.Y. Li, Y.J. Zhang, H.D. Fu, H.D. Huang, Q.F. Lu, H.J. Qin, et al., Hes1 knockdown exacerbates ischemic stroke following tMCAO by increasing ER stress-dependent apoptosis the PERK/eIF2α/ATF4/CHOP signaling pathway, Neurosci. Bull. 36 (2) (2020) 134–142, https://doi.org/10.1007/s12264-019-00411-7.

[45] G.E. Karagöz, D. Acosta-Alvear, P. Walter, The unfolded protein response: detecting and Responding to fluctuations in the protein-folding capacity of the endoplasmic reticulum, Csh Perspect Biol 11 (9) (2019) a033886, https://doi.org/10.1101/cshperspect.a033886.

[46] P. Habib, A.S. Stamm, J.B. Schulz, A. Reich, A. Slowik, S. Capellmann, et al., EPO and TMBIM3/GRINA promote the activation of the adaptive Arm and Counteract the terminal Arm of the unfolded protein response after Murine Transient cerebral ischemia, Int. J. Mol. Sci. 20 (21) (2019) 5421, https://doi.org/10.3390/ijms20215421.

[47] L. Yu, S. Li, X. Tang, Z. Li, J. Zhang, X. Xue, et al., Diallyl trisulfide ameliorates myocardial ischemia-reperfusion injury by reducing oxidative stress and endoplasmic reticulum stress-mediated apoptosis in type 1 diabetic rats: role of SIRT1 activation, Apoptosis 22 (7) (2017) 942–954, https://doi.org/10.1007/s10495-017-1378-y.
[48] S.Y. Yi, K. Chen, L.H. Zhang, W.B. Shi, Y.X. Zhang, S.B. Niu, et al., Endoplasmic reticulum stress is involved in stress-induced Hypothalamic neuronal injury in rats via the PERK-ATF4-CHOP and IRE1-ASK1-JNK pathways, Front. Cell. Neurosci. 13 (2019) 190, https://doi.org/10.3389/fncel.2019.00190.
[49] S. Matsumoto, M. Murozono, M. Kanazawa, T. Nara, T. Ozawa, Y. Watanabe, Edaravone and cyclosporine A as neuroprotective agents for acute ischemic stroke, Acute Med Surg 5 (3) (2018) 213–221, https://doi.org/10.1002/ams2.343.
[50] C. Li, Z. Mo, J. Lei, H. Li, R. Fu, Y. Huang, et al., Edaravone attenuates neuronal apoptosis in hypoxic-ischemic brain damage rat model via suppression of TRAIL signaling pathway, Int. J. Biochem. Cell Biol. 99 (2018) 169–177, https://doi.org/10.1016/j.biocel.2018.03.020.
[51] H. Ren, L. Ma, X. Gong, C. Xu, Y. Zhang, M. Ma, et al., Edaravone exerts brain protective function by reducing the expression of AQP4, APP and Abeta proteins, Open Life Sci. 14 (2019) 651–658, https://doi.org/10.1515/biol-2019-0074.
[52] A.A. Mohsin, J. Thompson, Y. Hu, J. Hollander, E.J. Lesnefsky, Q. Chen, Endoplasmic reticulum stress-induced complex I defect: central role of calcium overload, Arch. Biochem. Biophys. 683 (2020) 108299, https://doi.org/10.1016/j.abb.2020.108299.
[53] D. Stegner, S. Hofmann, M.K. Schuhmann, P. Kraft, A.M. Herrmann, S. Popp, et al., Loss of Orai2-mediated Capacitative Ca(2+) Entry is neuroprotective in acute ischemic stroke, Stroke 50 (11) (2019) 3238–3245, https://doi.org/10.1161/STROKEAHA.119.025357.
[54] Y. Han, M. Yuan, Y.-S. Guo, X.-Y. Shen, Z.-K. Gao, X. Bi, Mechanism of endoplasmic reticulum stress in cerebral ischemia, Front. Cell. Neurosci. 15 (2021) 704334, https://doi.org/10.3389/fncel.2021.704334.